

Faceting and defaceting phase transitions of Pd/W(111)

Yu-Wen Liao,^{1,3} L. H. Chen,² K. C. Kao,² C.-H. Nien,² Minn-Tsong Lin,^{1,3} and Ker-Jar Song^{1,*}

¹*Institute of Atomic and Molecular Sciences, Academia Sinica, Taipei, Taiwan*

²*Department of Physics, National Central University, Zhongli City, Taoyuan, Taiwan*

³*Department of Physics, National Taiwan University, 106 Taipei, Taiwan*

(Received 20 May 2006; revised manuscript received 18 December 2006; published 27 March 2007)

We have studied the faceting and defaceting phase transitions of Pd/W(111). In apparent agreement with results of recent theoretical simulation [C. Oleksy, *Surf. Sci.* **549**, 246 (2004)], we find the fastest way to create the largest facets is to anneal at a temperature right below the temperature that the defaceting transition occurs. On the other hand, while the paths of faceting transitions show normal retardation as the cooling rate is increased, the paths of defaceting transitions show negligible dependence on the heating rate even if increased by 64-fold. Another notable observation is a phase separation of the surface into defaceted and faceted regions after long annealing time while there is more than enough Pd remaining to induce faceting of the whole surface. This leads us to the proposal that instead of thermal disorder, the observed defaceting transition of the Pd/W(111) system is mainly driven by local loss of Pd, which is due to thermal desorption. Such desorption loss could be effectively replenished via surface diffusion at the vicinity of the Pd 3*d* islands. The observed independence of the defaceting transition path on the heating rate is rationalized as the consequence of a balance in between the loss and the supply of Pd, which can establish very quickly as the temperature rises.

DOI: [10.1103/PhysRevB.75.125428](https://doi.org/10.1103/PhysRevB.75.125428)

PACS number(s): 68.18.Jk, 68.35.Md, 68.43.Vx, 61.14.Hg

I. INTRODUCTION

Due to its potential application in forming nanostructures with interesting physical and/or chemical properties, adsorbate induced faceting has been studied extensively.^{1,2} In such studies, an adsorbate is used to enhance the surface energy anisotropy, which then provide the thermodynamic driving force that induces massive reconstruction of the substrate structure to expose facets of certain crystallographic orientations of high stability. Recently, adsorbate induced faceting has been utilized to change the shape of very sharp metal tips.³⁻⁵ Faceting of the Pd/W(111) system, in particular, has been demonstrated as a practical and easy way to reproducibly prepare well-characterized single atom tips^{6,7} which may be useful as tips for scanning tunneling spectroscopy or as highly localized field emission sources of electrons useful in ultrahigh resolution electron microscopy. As the surface energy anisotropy generally decreases with increasing temperature, the driving force for facet formation will reduce to zero at a certain temperature. For preparation and operation of such faceted tips, one obviously needs to know this temperature, above which defaceting will occur and the sharp faceted tips will become rounded. Although a lot is known about faceting of the Pd/W(111) system, the defaceting phase transition of Pd/W(111) has not been observed before this study.

Previous studies have established that a minimum coverage of about one physical monolayer (PML)⁸ of Pd is required for inducing faceting of W(111), which exposes {112} oriented facets. For coverage above 1 PML, it is known that the additional Pd tends to agglomerate into 3*d* Pd islands when annealed, leaving large part of the surface covered with a wetting layer of 1 PML, which induces faceting. This characteristic makes the preparation of a tip relatively easy, as there is no stringent requirement on the starting amount of Pd covering the W surface. For both W(111) and W(112) covered by a multilayer of Pd, it has been found that W can

diffuse into the Pd but not to the outer most physical monolayer.⁹⁻¹¹ Thus the Pd 3*d* islands should have some W atoms dissolved into it. It has also been observed that small pyramids with {110} oriented facets can form¹² among the {112} oriented facets when annealed for a long time. Earlier theoretical works^{13,14} have calculated the zero temperature surface energies of tungsten surfaces covered with various adsorbates and confirmed that 1 PML of some adsorbates (including Pd) can indeed enhance the surface energy anisotropy to provide the thermodynamic driving force for facet formation. Recently, Oleksy¹⁵ has addressed several very practical aspects of the temperature dependence of the faceting phenomena by using a solid on solid model and Monte Carlo simulation. Of particular interest are his demonstrations that the faceting-defaceting transition is of first order, the growth rate of facet size vs annealing temperature, the hysteresis in the faceting-defaceting phase transitions, the microscopically rough nature of the defaceted surface and a phase diagram as a function of temperature and the “effectiveness” of the adsorbate. Oleksy’s work certainly provides us a strong motivation to examine in detail the faceting-defaceting transition. It turned out that our findings about the growth rate of facet size as a function of annealing temperature is consistent with Oleksy’s prediction.¹⁵ But we also find features not accountable within the scope of Oleksy’s study which assumes constant coverage of 1 PML for both the faceted and the defaceted surfaces. In particular, both thermal desorption and surface diffusion of Pd are found to be integral parts of the phenomena and their interplay at the presence of Pd 3*d* islands can result in quite peculiar features such as heating rate independent path of defaceting transition.

Another unanticipated finding is a reversible change of Pd’s Auger signal associated with the defaceting-faceting transition. Although there is some ambiguity as to what causes it exactly, the finding forces us to reconsider the validity of the assumption that the coverage of the wetting

layer is the same on both the faceted and the defaceted surface.

II. EXPERIMENT

The experiment is performed in a UHV chamber (base pressure 8×10^{-11} torr) that has been described previously.¹⁶ Briefly, it is equipped to perform temperature programmed thermal desorption spectroscopy (TPD), temperature programmed Auger spectroscopy (TPA) and also temperature programmed low energy electron diffraction (TPLEED) studies. The W(111) crystal is provided by Surface Preparation Laboratory with a specified mosaic spread of less than 0.25° . They are cut within 0.25° of the (111) direction and are 3 mm wide, 12 mm long, and 0.3 mm thick. The crystal is cleaned by repeated dosing of oxygen and flashing to 2000 K. The evaporator of Pd has been described before.¹⁷ In particular, temperature programmed thermal desorption spectra have been used every day to check the calibration of both the Auger sensitivity and the deposition rate.

To measure the sample temperature, we make use of the fact that the resistivity of a W single crystal is a linear function of temperature for temperatures larger than 100 K. We used a pair of 0.003 in. diameter Ta wires to pick up the voltage drop across two points 6 mm apart along the direction of the heating current. Using the known current and the voltage drop, the resistance and thus the temperature can be calculated. We estimate the accuracy of the temperature is 5% at 1200 K, while the precision is about 1 K.

The temperature programmed and gated heating of the sample and detection of the LEED patterns has been described before.¹⁷ What is different in this study is the use of a CCD camera to record the LEED pattern. As the CCD camera is sensitive to near IR radiation from the heated sample, we used a high pass optical filter to suppress part of the IR background caused by the thermal radiation of the sample. In addition, we find and remove the temperature dependent residual background due to thermal radiation by monitoring an area on the LEED pattern that does not have any diffraction spot. The CCD camera we used allows us to record one LEED picture every 1.25 s, with 0.5 s for exposure and 0.75 s for digitization. At the maximum heating rate of 8 K/s we used, each image is an average from $T - 2$ K to $T + 2$ K and the image is assumed to represent the situation at the central temperature T .

III. RESULTS

A. The thermal desorption of Pd from W(111)

Figure 1 shows the desorption traces of Pd films from W(111) with various initial coverage. Consistent with previously published results,⁶ the spectra consists of a broad “monolayer” peak at about 1600 K and a “multilayer” peak at about 1300 K. Note that for the multilayer peaks, a common leading edge emerges as the coverage increased above 1 PML. Of particular interest in this experiment are the thermal desorption that occurs below 1200 K. Note that in between 1050 K and 1200 K, the desorption rate is not negligible, with a maximum value of about 0.01 PML/s at

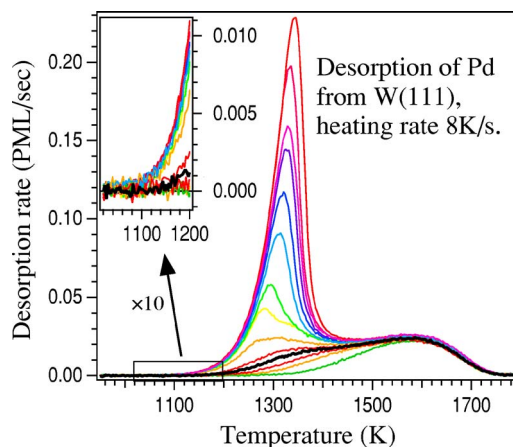


FIG. 1. (Color online) Desorption rate of Pd from various Pd films on W(111) with initial coverage ranging from 0.65 to 3.2 PML. Heating rate is 8 K/s for all curves. The thick (black) curve is of a film most close to 1 PML initial coverage. The inset shows a blow up ($\times 10$) of the leading edges.

1200 K for thick films. By integrating the common leading edge of the desorption curves, we can estimate the maximum amount of Pd thermally desorbed during the annealing process. In particular, for the thick films, if the heating-cooling rate is 2 K/s, then one full cycle in between 900 and 1200 K would cause a loss of 0.46 PML of Pd. For cycles with other constant heating-cooling rate, the amount of desorbed Pd is inversely proportional to the rate. Note: for the rest of the paper, when we refer to heating-cooling cycles, it always means cycling in between 900 K and 1200 K using a certain constant heating-cooling rate.

B. The apparent thickness of Pd on W(111)

We have measured the dependence of the Pd and W Auger signals as a function of thickness for a series of uniform Pd films (not shown). Consistent with a previously published result,⁸ we find the Auger signal S of the Pd to follow a form of $S = A[1 - \exp(-\alpha \cdot d)]$, in which d is the thickness and α the effective decay constant. Once we know A and α , the thickness d of a uniform film can be obtained if we know the Auger signal S , that is $d = -[\ln(1 - S/A)]/\alpha$. Even if the film is not uniform, we can still define $d_A \equiv -[\ln(1 - S/A)]/\alpha$ to be the film’s “apparent thickness,”¹⁶ which is just a linearized form of Auger. Since it is much easier to interpret, we will show all our temperature programmed Auger data in this “linearized” form below. Operationally, α need be determined only once. The value of A , however, is measured daily to ensure proper normalization.

Figure 2 shows the evolution of the apparent thickness^{16,18} of various Pd films (deposited at 130 K) when they are subject to the same annealing process. One can roughly separate Fig. 2 into two regions; the first part is when the sample is below 900 K. In this region, the Pd Auger signal of films thinner than 1.2 PML are stable, while that of the thicker films show decreases which have been attributed⁸ to agglomeration of Pd into $3d$ Pd islands. It is clear from Fig. 2 that there are some interesting metastable

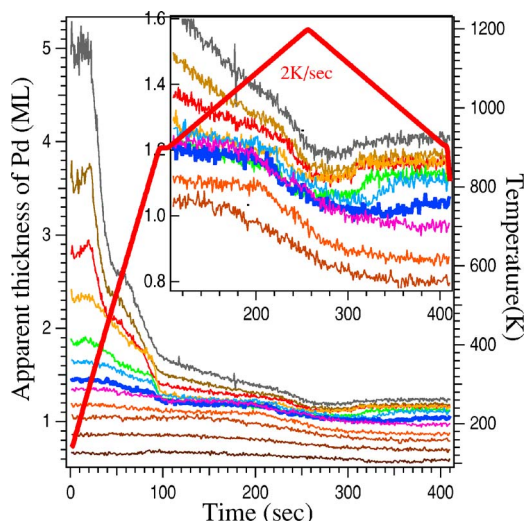


FIG. 2. (Color online) The apparent thicknesses of Pd as functions of time when films with various initial coverage are annealed using the same temperature program. The thick piecewise linear (red) line is the measured temperature as a function of time. To more clearly show the reversible dip near the maximum temperature, the inset shows part of the same data with an enlarged vertical scale.

features in the agglomeration process, but we will not discuss them in this paper. We do note that the agglomeration process is rather slow¹⁶ and continues to proceed at temperatures above 900 K. In addition to agglomeration, something else occurs at about 1100 K (~240 s on time scale) which accelerates the decrease of the apparent thickness. More surprisingly, for all films initially thicker than about 1.7 PML (i.e., all curves in Fig. 2 above the one with triple thickness), such decrease can later be recovered when the temperature is lowered. As will be shown below, these recoverable dips are due to reversible defaceting-faceting transition of the surface. Recall that the estimated thermal desorption loss of Pd is 0.46 PML for one heating-cooling cycle. Within experimental uncertainty, this is consistent with the observation that for films with initial coverage smaller than 1.5 ML, the decrease of the apparent thickness will not recover at all. For films with initial coverage near 1.7 PML, the exact amount recovered and the temperature this occurs depends on the initial coverage. We attribute such behavior to reduced density of the surviving Pd 3d islands.

C. The phase transition as observed by temperature programmed low energy electron diffraction and temperature programmed Auger

The nature of the reversible dip in the apparent thickness of Pd is better revealed by observing the LEED pattern of a sample prepared and annealed in identical ways as that in a TPA measurement. Figure 3 shows the result of such an experiment with Pd films of 2.35 PML initial coverage. Figure 3(a) shows all the quantities as functions of time during the later part of the annealing process, which consists of two 2 K/s heating-cooling cycles. The “estimated coverage” is the calculated average coverage of Pd remaining on the sur-

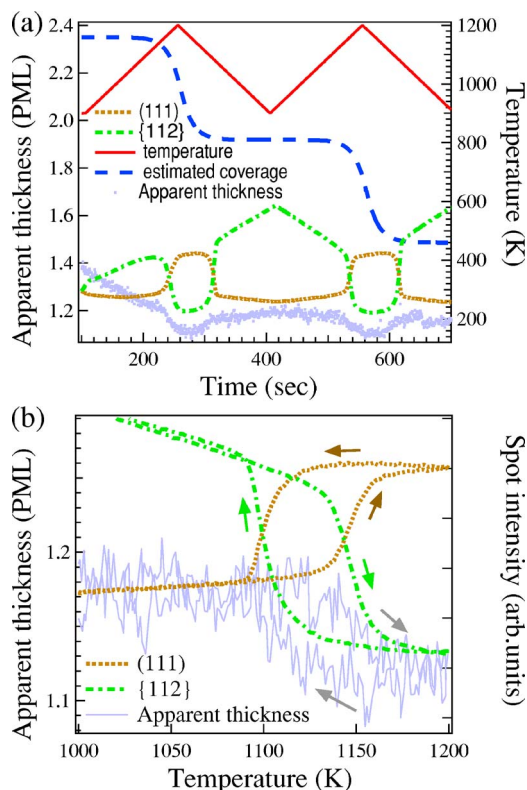


FIG. 3. (Color online) (a) Time dependence of measured temperature, apparent thickness of Pd and intensity of the LEED spots during an annealing experiment with two heating-cooling cycles. The “(111)” and “{112}” are the intensities of the LEED spots originated from the (111) planar and {112}-faceted surface, respectively. (b) The apparent thickness and the intensity of the LEED spots plotted as functions of temperature for the intermediate cooling-heating cycle (1200 K → 900 K → 1200 K). All three curves clearly show hysteresis.

face. The calculation assumes that the only loss mechanism of Pd is due to thermal desorption, which is assumed to follow zero order desorption kinetics as mentioned previously. The difference between the estimated coverage and the apparent thickness, i.e., Pd invisible by Auger, should be hidden underneath the Pd 3d islands. The “(111)” and “{112}” are the intensities of the LEED spots originated from the (111) planar and {112}-faceted surface, respectively. As has been observed before,⁸ the as-deposited surface remains planar and faceting can occur only when the temperature is raised. The feature we find is the reversible transition between the faceted and the defaceted surface, as indicated by the dips in the {112} (green) curve and the corresponding bumps in the (111) (brown) curve. Although reversible, the transition has hysteresis, which is made obvious in Fig. 3(b). Here, the same data are plotted as functions of the sample temperature during the intermediate cooling-heating cycle (1200 K → 900 K → 1200 K). The arrows indicate the direction of time. Hysteresis is obvious in either the intensities of the LEED spots or the apparent thickness. The width of the hysteresis (measured across the half-way points) is about 45 K, which is about 4% of the faceting transition temperature. In comparison, this ratio is about 2% for the

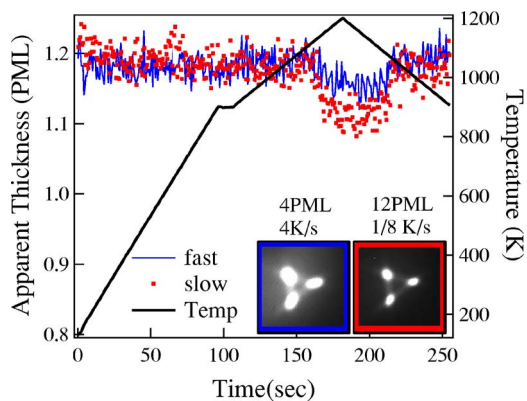


FIG. 4. (Color online) The inset shows the LEED patterns of two samples prepared by either “fast” annealing (4 K/s) or by very “slow” annealing (1/8 K/s). The figure shows the apparent thickness of the two samples as functions of time when undergoing identical subsequent annealing processes (4 K/s).

Pd/Mo(111) case¹⁷ and 6% in Oleksy’s simulation.¹⁵ One also notes that the dips in the apparent thickness correlate very well with the dips and bumps in the intensity of the LEED spots. This suggests very strongly that the downs and ups in the apparent thickness are associated with the defaceting and faceting phase transitions.

D. Dependence of the depth of the Auger dips on sample preparation

The effect of annealing time is shown in Fig. 4. To compensate for the difference in the amount desorbed during the annealing process, different initial amount of Pd (4 and 12 PML) is deposited. The sample is then subjected to two annealing cycles, the first one is at 4 K/s, while the second one is either “fast” (4 K/s) or very “slow” (1/8 K/s). Figure 4 shows the LEED patterns of the samples thus prepared. Also shown are the apparent thicknesses of the two samples as functions of time when subsequently undergoing identical annealing processes. One can clearly see that for the very slowly annealed sample (red dots), not only the LEED spots are about 2 times sharper; the dip in Pd’s apparent thickness is also about 2 times as deep.

E. Growth of the facet size as a function of the annealing temperature

Generally, one would expect that given a fixed annealing time, annealing at a higher temperature should result in facets with larger average size. However, when there is a defaceting transition, it is obvious that one should not anneal at too high a temperature such that the sample is in a defaceted planar state. But what is the best temperature for annealing if we want to get the largest size in the shortest amount of time? According to Oleksy’s simulation,¹⁵ the best annealing temperature should be the maximum temperature that does not cause defaceting transition to occur. Figure 5 shows results of an experiment to test that prediction. A series of samples were prepared with 3 PML of Pd deposited at 130 K, annealed at a temperature ranging from

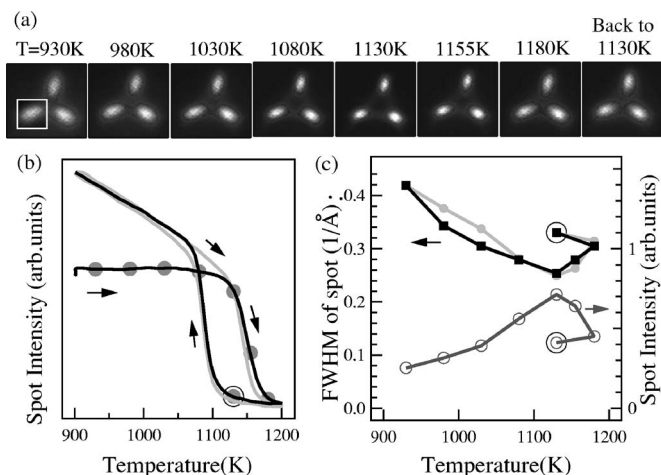


FIG. 5. (a) LEED patterns of a series of samples after they had been annealed at the indicated temperatures for 30 seconds and quenched down to 130 K. The last pattern labeled “back to 1130 K” is of a sample that is first heated to 1200 K and then lowered to 1130 K for annealing. (b) The intensity of a {112} associated LEED spot as a function of temperature during two consecutive annealing cycles is first measured. The annealing temperatures (solid circles) are then selected based on results of the first cycle (the dark curve). (c) The full width at half-maximum W (black solid square) measured along the long axis, and the integrated intensity I (open circle) of the lower left LEED spots shown in (a). The “back to 1130 K” point has been emphasized with a big empty circle. The gray solid circles are plot of $\alpha I^{-1/2}$. As shown, the width W of the LEED spot is approximately proportional to $I^{-1/2}$, meaning the facet size are smaller than the transfer width of the LEED electron beam. The lines connecting neighboring data points are guides for the eyes only.

930 K to 1180 K and then quenched. The LEED patterns of these cooled samples are shown in Fig. 5(a). The relation of the chosen annealing temperatures relative to the defaceting-faceting transition paths are shown in Fig. 5(b), while the integrated intensity and width of the LEED spots of the annealed samples are shown in Fig. 5(c). Note that the sharpest spot and thus the largest average facet size are obtained by annealing at 1130 K. As this is the temperature that corresponds to the onset of the defaceting transition, our result seems to confirm Oleksy’s prediction.

Note that annealing above 1130 K causes the observed facets to reduce in size. Presumably, our quenching is not fast enough to freeze the surface in a defaceted state and faceting occurred during cooling. Of particular interest is the last case labeled “back to 1130 K.” It is of a sample that is first “over” heated to 1200 K and then cooled to 1130 K for annealing. The intensity and width of the spot is about the same as that of the “1180 K” case, which corresponds to significantly smaller size of facets compared with that of the “1130 K” case. This indicates the effect of annealing depends strongly on the state of the surface itself. In the “1130 K” case, annealing of the faceted surface causes the facet size to increase. In the “back to 1130 K” case, however, the surface has become defaceted by being first raised to 1200 K. Presumably, as the surface remains defaceted after the temperature is lowered back to 1130 K, annealing at that

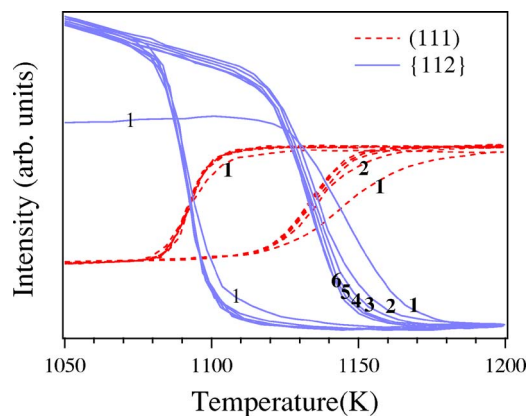


FIG. 6. (Color online) Result of a TPLEED experiment in which a sample with initial Pd coverage of 3 PML is subjected to six consecutive 4 K/s cycles of heating and cooling. “(111)” and “{112}” are the intensities of LEED spots associated with the (111) and {112}-faceted surface, respectively. The sequence numbers of the thermal cycles are marked on each corresponding curves.

temperature is of no effect. Like the 1180 K case, we believe the observed facets are generated during the transient cooling stage and thus facets of about the same size resulted in both cases. We note that such “bistable” behavior has also been predicted by Oleksy’s simulation.

F. Dependence of the transition path on the sequence number of the heating cycles: First cycle vs later cycles

What happens to the hysteresis if the sample is subjected to repetitive heating and cooling cycles? Figure 6 shows the result of a TPLEED experiment in which a sample with initial coverage of 3 PML is subjected to six consecutive 4 K/s cycles of heating and cooling. One obvious feature that is common to all the multiple thermal cycle experiments we have performed is that there is a relatively big difference between the transition path of the first cycle and those transition paths of all later cycles. In particular, the transition temperature is always higher for the first cycle. For later cycles, the transition paths tend to drift toward lower temperatures, but the differences are relatively small. Why is the first cycle distinctly different? One possibility is that some of the extra Pd has not yet been incorporated into 3d Pd islands. To check this possibility, one can deposit additional Pd onto a surface that has already undergone several cycles. The result is shown in the following experiment.

G. Dependence of the transition path on additionally deposited Pd

In this experiment, one first deposit 4 PML of Pd on a clean W(111) surface at 130 K and then subjects the surface to two 2 K/s heating-cooling cycles. Afterward, the surface is allowed to cool down to 130 K and additional 1 PML of Pd is deposited onto the surface, and the surface is subject to two more 2 K/s heating-cooling cycles (cycle 3 and cycle 4) and then cooled down. Finally, additional 2 PML of Pd is again deposited onto the surface (at 130 K), and two more

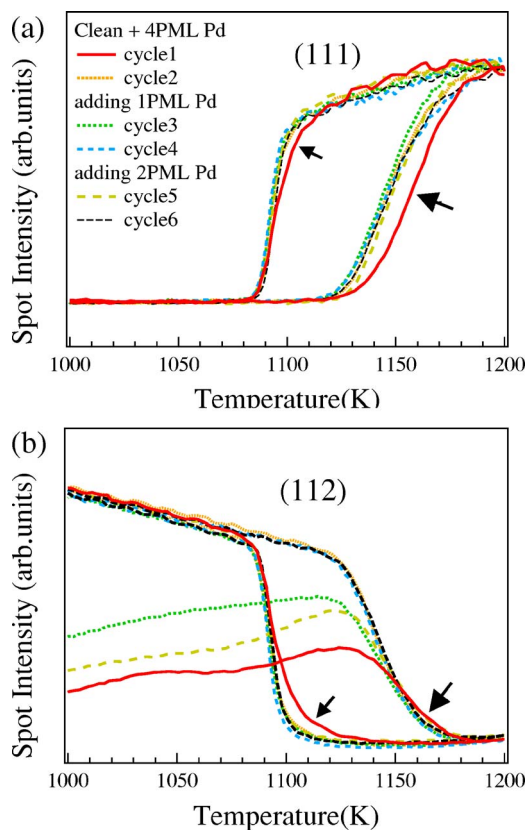


FIG. 7. (Color online) Intensities of LEED spots originated from (a) (111) and (b) {112}-faceted surface as the sample is subjected to three sets of double heating-cooling cycles. Legends of (a) also applies to (b). 4 PML of Pd were deposited onto the surface initially while additional 1 and 2 PML of Pd was deposited in between successive set of double cycles. From (b), one can see that each deposition caused significant change in the intensity of the {112} originated LEED spots. But it is obvious from (a), that there is something special (indicated by the arrows) about the very first annealing cycle after the initial deposition. The transition path for that “virgin” cycle cannot be reproduced by adding additional Pd onto the annealed surface.

2 K/s heating-cooling cycles (cycle 5 and cycle 6) are applied to the surface. The intensities of (111) and {112} associated LEED spots as functions of temperature during all the heating-cooling cycles are shown in Figs. 7(a) and 7(b), respectively. From Fig. 7(b), one notices that the more there are Pd in excess of the wetting layer, the lower the intensity of the {112} spot immediately after deposition. However, one notices from both Fig. 7(a) and 7(b) that for cycle 3 and cycle 5, once the newly deposited Pd has been annealed to 1150 K, the transition path afterwards become nearly the same as those of cycles 2, 4, and 6. That is, although deposition of additional Pd caused significant reduction of the intensity of {112} LEED spot initially, little or no influence is left when the (111) spots start to show up. In contrast, the transition path for cycle 1 is significantly different (indicated by the arrows) from the rest of the cycles even after being annealed to 1200 K and is cooling down. Whatever makes the first annealing unique, it cannot be regenerated simply by depositing more Pd to the surface.

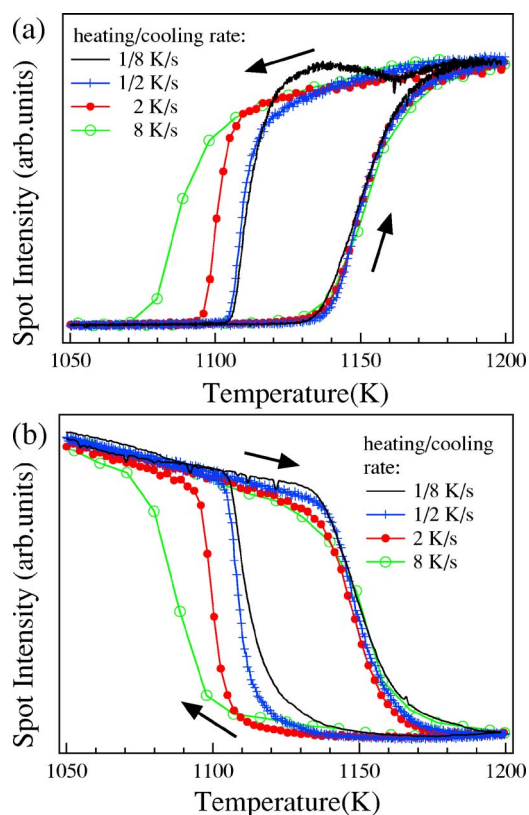


FIG. 8. (Color online) Intensities of the LEED spots associated with (a) (111) and (b) {112}-faceted surface are plotted as functions of temperature for samples subjected to different heating-cooling rates (see text for detail). Note the negligible dependence of the transition paths on the heating rate for the defaceting transitions, in contrast with the strong dependence of the paths on the cooling rate for the faceting transitions.

H. Negligible dependence of the path of transition on the heating rate

Due to finite response speed of a material system, one expects the observed path of transitions will depend on the heating or cooling rate. The “intrinsic” transition temperature can only be found when the heating-cooling rate is small enough. Oleksy’s simulation also predicts a very sharp transition in temperature when the heating rate is small. It is thus very interesting to know how the path of transition depends on the heating or cooling rate. As the surface is in some kind of unsettled state during the first annealing cycle, we try to avoid that complication by studying only later annealing cycles. The results of four experiments were shown in Fig. 8. For each experiment, 13 PML of Pd was deposited onto the clean W(111) surface while the sample is held at 800 K. The samples thus prepared are then subject to two heating-cooling cycles. The first cycle is always a 4 K/s cycle, while the rate of the second cycle is x K/s, where “ x ” is one of {1/8, 1/2, 2, 8}. The integrated intensity of a (111) associated LEED spot during each of the second annealing cycles is shown in Fig. 8(a), while that of a {112} associated LEED spot is shown in Fig. 8(b). From these figures, it is clear that the path of faceting transition has a significant dependence on the cooling rate, which seems normal. The paths of de-

faceting transitions, however, show little change as the heating rate is varied from 1/8 K/s to 8 K/s. Also, the defaceting transitions do not become more abrupt in temperature as the heating rate becomes much slower. As this is totally unexpected, we have done similar experiments many times and the defaceting transitions (of the second and later cycles) always show little dependence on the heating rate. This means that during heating, the defaceting surface responds so quickly that it can keep up with the largest heating rate, but instead of going all the way to complete the transition, the surface somehow will stay in some kind of temperature dependent intermediate states. If these intermediate states were a sequence of equilibrium states, then one would expect the system to follow the same path backward when the temperature is lowered. But the existence of hysteresis clearly contradicts this hypothesis. That the system can behave like this puzzled us for quite some time until we make the following serendipitous observation.

I. Inhomogeneity of the wetting layer induced by high temperature annealing

Ordinarily, one would expect when the coverage is more than 1 PML, there will be Pd $3d$ islands sitting on top of a uniformly wetted surface (with coverage of 1 PML). We find accidentally, however, the coverage of the Pd wetting layer can become inhomogeneous after long time annealing at high enough temperature. A sample of 3 PML of Pd was annealed at 1100 K for 30 minutes and then quenched to 130 K. After quenching, the LEED pattern indicates coexistence of both (111) and {211} spots, as shown in Fig. 9(a). This is a surprise as the annealing temperature is below defaceting transition and we have estimated before annealing that there should be about 1.6 PML of Pd left on the surface after annealing, which should be plenty to keep the whole surface wetted and thus fully faceted. The defaceted part must be due to lack of Pd. It seems that thermal desorption has caused part of the surface to assume a coverage less than the critical coverage needed for inducing faceting and quenching prevented the surface diffusion from bringing the coverage back to 1 PML. Annealing this surface again at slightly lower temperature of 1050 K for 2.5 minutes, however, resulted in a fully faceted surface, as shown in Fig. 9(b). To directly measure the average coverage after the initial annealing, another sample is prepared in the same way. We again observed LEED pattern similar to that shown in Fig. 9(a). Thermal desorption spectra of this surface is then obtained and shown as the solid curve in Fig. 9(c). It clearly has a multilayer peak and integration indicates the total amount of Pd to be 1.45 PML, in reasonable agreement with our initial estimate.

J. Dependence of the path of transition on the sample temperature during deposition

One generally expects that growth at higher substrate temperature will result in $3d$ islands of larger size but lower density. It is thus interesting to study whether the transition path has any dependence on the substrate temperature during the film’s deposition. Three different samples were prepared

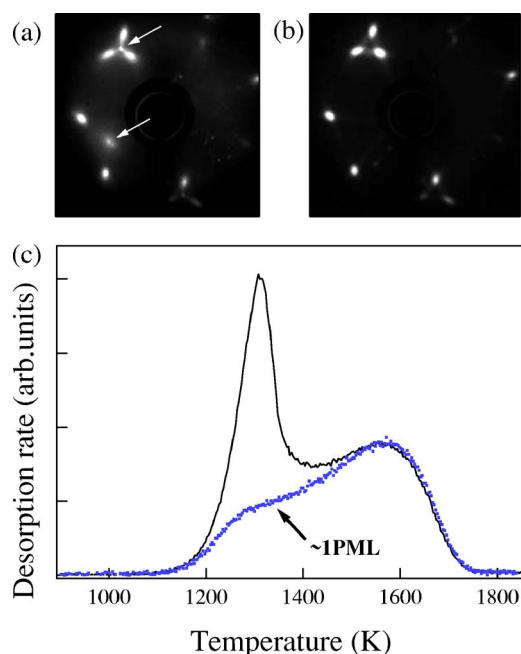


FIG. 9. (Color online) (a) LEED pattern of a sample with initial coverage of 3 PML Pd, after being annealed for 30 minutes at 1100 K and then quenched to 130 K. Diffraction spots from (111) planar surface, as indicated by the arrows, are clearly seen. (b) The surface became fully {112}-faceted after being annealed again at 1050 K for 2.5 minutes. (c) The thermal desorption spectra (the solid black curve) of a surface prepared in identical ways as the surface shown in (a). There was about 1.45 PML of Pd under the solid curve. The thermal desorption spectra of a surface with nearly 1 PML coverage of Pd (the blue dots) is shown for comparison.

with the sample temperature held at 130 K, 800 K, and 1050 K, respectively, during deposition of 4 PML of Pd. After deposition and cooling down to 130 K, each of these samples is then subject to two consecutive heating-cooling cycles (at 2 K/s) while its LEED patterns are recorded. The integrated intensity of a (111)-associated diffraction spot is measured and shown in Fig. 10. It is obvious that the higher the sample temperature during deposition, the less the difference between the paths of transition between the first annealing cycle and the second annealing cycle. For deposition at 1050 K, the difference practically disappears.

IV. DISCUSSION

A. The defaceting transition

The experiment as shown in Fig. 9 clearly demonstrates that whether the wetting layer becomes inhomogeneous depends critically on the annealing temperature. It strongly suggests that, on a surface populated with 3d islands, the interplay of the thermal desorption and the surface diffusion may cause a lot of the observed features. We now discuss some aspects of this interplay.

Consider the case in which there is only one 3d Pd cluster on a fully wetted surface. Assume the sample is heated up to a temperature with significant thermal desorption. Although the Pd 3d island can serve as a source and replenish some of

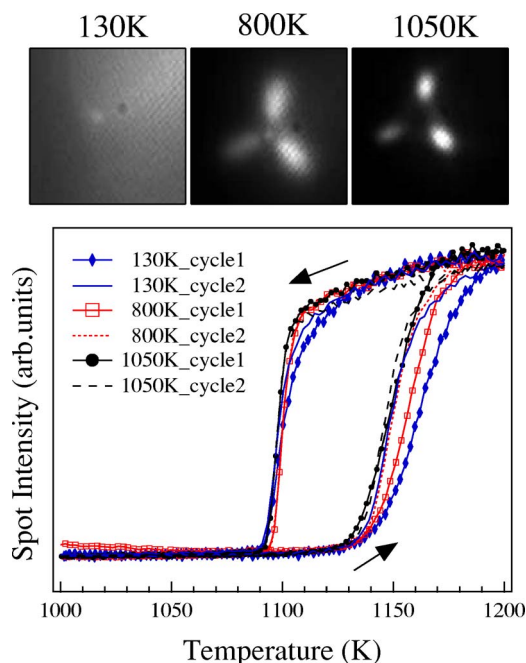


FIG. 10. (Color online) On the top are the LEED pictures of three samples right after preparation by depositing 4 PML of Pd while the samples were held at temperatures of 130 K, 800 K, and 1050 K, respectively. These samples are then subject to two consecutive 2 K/s heating-cooling cycles. Intensity variation of one (111) associated LEED spot as functions of time are shown in the bottom. Transition temperatures for all the second cycles are nearly the same. But, for the 130 K-deposited sample, the defaceting transition path (solid blue diamonds) for the first annealing cycle is about 13 K higher than that for the second annealing cycle. For the 800 K-deposited sample (red empty square), the difference is about 7 K. For the 1050 K-deposited sample (solid black circle), the difference is negligible.

the loss of a nearby area via surface diffusion, it cannot maintain the same coverage at places far away. Assuming a “steady” state profile is reached before the Pd 3d cluster is exhausted, then one can imagine there is a protected neighborhood within which the coverage is high enough and the surface remains faceted, while places outside become depleted in Pd that the surface become planar. The size of the “protected” neighborhood will depend on the strength of the loss mechanism (thermal desorption) relative to that of the supply mechanism (surface diffusion).

If, for places not covered by the 3d cluster, we assume the diffusion constant D to be independent of the coverage and the rate of thermal desorption to be first order, then the partial differential equation governing the coverage would be $\frac{\partial \theta}{\partial t} = D \nabla^2 \theta - \frac{\theta}{\tau}$. Note that τ is the mean lifetime of Pd on the surface due to desorption when no Pd 3d island exists. We note that for such an equation, a time independent steady state must satisfy $\nabla^2 \theta = \frac{\theta}{D\tau}$. This means that the length scale is determined by $\sqrt{D\tau}$. In particular, the size of the protected region should be proportional to $\sqrt{D\tau}$. Note that τ is proportional to $e^{E/(kT)}$, while D is proportional to $e^{-d/(kT)}$, where E and d are the activation energies for desorption and diffusion respectively. $\sqrt{D\tau}$ is thus proportional to $e^{(E-d)/(2kT)}$.

There is an empirical correlation which claims that the energy barrier of surface diffusion amounts to about one-tenth the heat of sublimation of the atoms in their solid state.²⁰ The activation energies of terrace diffusion for Pd on W(111) (Ref. 21) and W(211) (Ref. 22) are 1.02 ± 0.06 eV and 0.34 ± 0.01 eV, respectively. The activation energy for thermal desorption of bulklike Pd from W(111) (Ref. 8) is 3.76 ± 0.4 eV. The general trend of desorption traces as shown in Fig. 1 is similar to the case of Pd/Mo(111),²³ one thus expects the activation energy for the desorption of Pd from the physical monolayer will be in between 4.13 and 5 eV. Although the coverage dependence of the activation energies for the Pd/W(111) case has not been reported, one does expect the activation energy of surface diffusion to be always much smaller than the activation energy of desorption. As a result, the size of the protected region, which is proportional to $\sqrt{D\tau}$ and thus $e^{(E-d)/(2kT)}$, will be a strongly reducing function of T . Although thermal desorption is generally totally negligible at low temperature, its significance (relative to that of the surface diffusion) increases quickly as temperature increases. This should be the reason behind the sensitive temperature dependence shown in Fig. 9. Using the above activation energies for Pd, we estimate the radius of a protected region at 1050 K should be about 2.4 to 2.6 times that at 1100 K and 5.2 to 6.2 times that at 1150 K.

The experiment in Fig. 9 suggests the possibility that the defaceting transition we observed may be caused by reduction of local Pd coverage. One crucial question is how fast could the inhomogeneity in coverage build up, when the temperature is raised? Note that for the partial differential equation we just described, a sinusoidal profile with wave vector k will decay exponentially with a time constant of $\frac{\tau}{1+D\tau k^2}$. Whatever k might be, this is always shorter than τ . This means that small deviation from steady state profile will decay on a time scale shorter than τ . Since τ is proportional to $e^{E/(kT)}$, it decreases even more strongly than $\sqrt{D\tau}$ as temperature increases. Using 4.13 eV as activation energy for thermal desorption, $\tau(1150)$ is approximately 1/50 that of $\tau(1050)$. Since $\tau(1050)$ should be a fraction of 150 s, $\tau(1150)$ is a fraction of 3 s. This is consistent with the fastest transition path in Fig. 8, which would suggest $\tau(1150)$ to be less than 1 s. Although more detailed comparison is not possible at this moment, we can say that the qualitative trend of much faster response time at higher temperature is consistent with our experimental observation.

The effectiveness of surface diffusion in replenishing the loss caused by thermal desorption should depend not only on the temperature but also on the density of the 3d Pd islands. The higher the island density n , the smaller the critical radius R of each protected region need be in order to cover the whole surface. We have $n \sim R^{-2} \sim (D\tau)^{-1} \sim e^{-(E-d)/(kT)}$, where T is the temperature where the radius of protection equals R . Above T , some part of the surface will not have adequate protection and become faceted. Since $e^{-(E-d)/(kT)} \sim n$, T is an increasing function of n .

In most of our experiments, we deposited the Pd at 130 K and then annealed to induce agglomeration, which initiates at about 300 K. The density of clusters produced this way should be very high at about 300 K. Annealing to higher

temperature generally caused coarsening of the clusters. As shown in the inset of Fig. 2, the apparent thickness is clearly decreasing before the first defaceting transition, indicating significant rate of coarsening. As can be seen in Fig. 3, the declining trend of the apparent thickness ceases after the first heating-cooling cycle. Our experience¹⁶ with Ag clusters indicates that the density of the 3d clusters depends much more on the maximum temperature the film has ever been annealed up to, and to a lesser degree also on the heating rate and/or annealing time. Presumably, coarsening at the maximum temperature quickly reduces the density of the clusters. Once the 3d clusters are far enough from each other, their mutual interaction via either a 2d gas or a direct encounter is reduced, and thus the observed reduced rate of further change.

The higher defaceting transition temperature for the first heating process as shown in Fig. 6 is naturally explained as a result of higher density of the 3d islands during the initial heating process, the much smaller changes in the defaceting temperature can also be rationalized as due to reduced changes in the density of the 3d islands. The results in Fig. 10 provide further qualitative support that the defaceting transition temperature depends on the density of the 3d island. As expected, the lower the sample temperature during deposition, the higher the density of the 3d islands formed and the higher the temperature of transitions for the “virgin” annealing. After being raised to 1200 K once, however, all samples behave about the same as the island densities become about the same.

For the second and later cycles, the independence of the defaceting transition path on the heating rate and the non-abrupt nature of the defaceting transition is also comprehensible if we assume the density of the 3d Pd islands remains the same during the heating process. Defaceting will start from areas on the surface that become depleted in Pd first, presumably regions far away from all the 3d islands. The depleted and thus defaceted region will increase as temperature increases. This should be the reason why the defaceting transition is not abrupt (in temperature). Also, with the density of the Pd islands remain the same, so long as the “steady” state coverage distribution can be reached quickly, the total protected area will depend only on the temperature. Under such circumstance, the apparent transition path will also depend only on the temperature and be independent of the heating rate. This is just what we observed. We thus propose that the defaceting we observed is driven by local loss of Pd and the peculiar heating rate independence of the defaceting transition path to be the result of a dynamic balance of thermal desorption and surface diffusion.

Finally, it seems that the larger depth of the dip in the apparent thickness of Pd for an extremely well annealed surface may be rationalized as a result of very small density of Pd 3d islands, which would allow larger areas to become depleted. Note, however, it is not clear why the dip in apparent thickness does not become deeper as the annealing temperature kept on increasing beyond the defaceting transition region. This seems to suggest that additional physical mechanisms may also participate in determining the depth of the dip. For example, one may wonder whether the dip is due to difference in scattering of Auger electrons by different local

geometry of (111) and {112} surfaces. As we have not seen similar dips for the defaceting-faceting phase transitions on Pd/Mo(111), we tend to believe that due to the large solid angle a CMA collects, differences in scattering is likely to be averaged out. Another possible cause of the dip to be discussed next is that the wetting layer on the defaceted surface prefer to assume a coverage different from 1 PML even if desorption is negligible.

B. Thermodynamic considerations

Conceptually, one can imagine a system, which consists of the inner walls of a cavity all composed of tungsten single crystals with (111) macroscopic orientation. Assuming diffusion of Pd into the bulk of tungsten is negligible, than such a cavity becomes a closed system. Given a certain amount of Pd, the Pd/W(111) can reach thermodynamic equilibrium with the Pd vapor. If the total amount of Pd is more than that needed to wet the whole surface and maintain a Pd vapor, then there could be Pd $3d$ islands condensed somewhere on the cavity wall. For such a closed system, effects of thermal desorption and deposition should balance each other and the surface concentration of Pd will reach maximum uniformity. If the temperature is then varied very slowly and uniformly over the whole sample, we expect the “intrinsic” defaceting-faceting transitions could be observed, which should be as abrupt as possible in temperature. To differentiate the faceting-defaceting transitions of such a closed equilibrium system from that of an open system (such as observed in our experiment), one may add “cavity” to designate the closed equilibrium system. For example, the defaceting transition on the wall of such a cavity will occur at a “cavity defaceting temperature,” which should be higher than the defaceting temperature we observed. Exactly how much higher is it? How will the cavity defaceting temperature depend on the coverage of Pd, especially when the average coverage is very slightly less than 1 PML? These are interesting but unsettled questions.

As 1 PML is the wetting layer for {112} surface, the maximum surface coverage for which a thermodynamic equilibrium state exists is 1 PML. Above 0 K, it seems that if Pd $3d$ islands exist, the desorption rate from the Pd $3d$ island will be larger than that from the exactly 1 PML wetting layer of Pd. In that case, Pd desorbed from the Pd $3d$ islands will condense on the wetting layer and a $2d$ gas will build up on top of the PML until a new desorption-adsorption balance is reached. The density of the $2d$ gas will depend on the energy difference between the binding sites on the wetting layer and those on the Pd drop. As 1 PML is the wetting layer, by definition, binding of extra Pd to sites on top of the PML is weaker than to sites on the Pd drop. The question is how much weaker. Unfortunately, we found no published calculation of this energy difference. Otherwise, one could estimate the density of the $2d$ gas. In general, one may guess that such binding should be stronger²⁴ to a rougher surface (i.e., 111) than to a smoother one (i.e., 112 or 110). Thus one may expect the equilibrium density of the $2d$ gas to be higher on the (111) than on the (112). Alternatively, if the Pd coverage is slightly less than 1 PML, then one needs to consider

the energy cost to create “holes” instead. This time, the cost will be higher on the smoother (112) than on the rougher (111) surface. Thus, at the same temperature, the equilibrium vapor pressure will be smaller for cavities with (112) walls than for cavities with (111) walls. If both (111) and (112) types of walls exist in the same cavity, then, under equilibrium, more of the holes will gather on the (111) surface than on the (112) surface. That is, to coexist in equilibrium, (111) must have a smaller coverage than (112). Although it is convenient for theoretical works to study and compare (111) and {112} surfaces with the same coverage, one needs to keep in mind that (111) surface with 1PML coverage is simply thermodynamically unstable.

Experimentally, the case of Pt/W(111) seems to be a most dramatic example. In this case, if the coverage of Pt is in between 2/3 and 1 PML, the Pt covered surface will phase separate into two regions, one with 1 PML coverage and faceted while the other region planar with coverage of 2/3 PML.^{25,26} That is, at 0 K, there is no homogeneous thermodynamic equilibrium phase with coverage in between 2/3 and 1 PML. Similar situations occur for Pd/W(111) (Ref. 8) and Pd/Mo(111),¹⁷ with much smaller coverage range for coexistence of both faceted and planar phases, being about 1/10 and 1/16 PML, respectively. That is, for all these systems, there are tendencies for the holes to segregate and form some kind of ordered planar (111) phase at low and medium temperature. But what happens close to the “intrinsic” defaceting transition? If not much happened, then one would expect a dip in the apparent thickness as the coverage of the wetting layer on (111) surface is smaller. This is in apparent agreement with the Pd/W(111) experiment. However, to reconcile with the Pd/Mo(111) case in which no dip is observed (with a noise about 0.04 PML), one must allow the possibility that the coverage of the Pd wetting layer on planar Mo(111) may approach that on the faceted surface at the transition temperature. The difference in the depth of the dips as shown in Fig. 4, however, cannot be accounted in a straightforward way. Future works measuring the density and size of the Pd islands and theoretical discussion about the planar-faceted phase boundary as functions of both coverage and temperature would be really helpful in fully clarifying the situation.

C. Asymmetry in the defaceting-faceting phase transitions

In our discussion of the defaceting process, one tacit assumption is that once the coverage of Pd decreases below a certain threshold, the surface becomes defaceted. Experimental results apparently support such a hypothesis. On the other hand, when it comes to faceting, the observed retardation seems to suggest faceting to be a significantly slower process. As shown in Fig. 8, faceting start to show sign of lagging behind at cooling rate of about 1/2 K/s, while defaceting shows sign of lagging behind at heating rate of 8 K/s. One thus estimates a 16-fold difference in the “speed” of the two processes. Although generally one would expect it to be easier to undercool than to overheat a system, the big disparity of surface diffusion of Pd on W(112) compared with that on W(111) may be a major contribution to the 16-fold dif-

ference. Recall that the activation energy for Pd surface diffusion on W(112) is 0.34 eV, which is much smaller than the 1.02 eV for diffusion on W(111). Together with the prefactors,^{21,22} this results in a 800-fold difference in the surface diffusion constants at 1100 K. Although the microscopic structure of the defaceted surface¹⁵ could be quite different from that of a planar W(111), presumably the surface diffusion constant of Pd on it will also be quite small compared with that on W(112) facets. As noted in Fig. 2, the recovering of the Pd Auger synchronizes with the faceting transition. It is thus certainly possible that the faceting transition is also mediated somehow by the competition between thermal desorption and surface diffusion, except now the surface diffusion is much slower. More quantitative modeling is currently being carried out and we will report the results in a separate paper.

D. Formation of single atom tips

In case one needs to use faceting to get a single atom tip, we imagine the first step is to make the front end of the tip a single pyramid. If the etched tip is not very small, multiple features such as hill and valley¹⁸ may occur. Figure 5 shows us that to get the largest facet size in the shortest time, the best annealing temperature is right below the defaceting transition temperature, i.e., at 1130 K. Note, however, the best temperature for getting a large single pyramid need not be the best temperature for obtaining a single atom tip. Nien and Madey have reported¹⁹ STM studies which indicate the edges of the pyramids (prepared at 1075 K) to be truncated and the apex rounded. Fu *et al.* have reported⁶ FIM studies, which indicate atomically sharp edges, and single atom apex for tips annealed at 1000 K. These studies suggest that the edge and the apex structure is very likely temperature dependent. In the case of oxygen induced faceting, Bryl and Szczepkowicz⁵ have used an annealing temperature of 1400–1600 K to obtain a single pyramid, while using an annealing temperature of 1000–1060 K to sharpen the tip. These suggest that the best annealing temperature for form-

ing sharp single-atom apices can occur at significantly lower temperature than that of the defaceting transition. A conservative strategy would be to form a single pyramidal tip first, and then to anneal at a lower temperature to sharpen the apex to a single atom configuration.

V. SUMMARY

We have studied the defaceting and faceting phase transitions of the Pd/W(111) system. As predicted by Oleksy, the growth of facet size is fastest at a temperature right below the defaceting temperature. A decrease of the Pd Auger signals occurs when the surface becomes defaceted. This decrease is reversible when the surface transforms back to a faceted one. We have found the path of defaceting phase transition to be surprisingly independent of the heating rate used. We have also found evidence indicating the Pd coverage on the surface can become inhomogeneous due to thermal desorption, which leads us to propose that the observed defaceting is initiated by lack of Pd at places where the thermal desorption loss cannot be efficiently replenished. The heating rate independent defaceting transition path is interpreted as a consequence of a temperature dependent quasi-steady state balance between the surface diffusion and thermal desorption. Finally, we try to point out that transport of Pd among different phases should be an important aspect of the phenomena and to fully understand the faceting-defaceting transition, it is not only necessary to consider the finite temperature effect, but also important to allow the coverage to vary from place to place.

ACKNOWLEDGMENTS

The authors acknowledge funding by National Science Council under Grants Nos. NSC-92-2112-M-001-039, NSC 93-2112-M-001-045, NSC 91-2112-M-008-057. One of the authors (K.J.S.) acknowledges interesting and stimulating discussion with Andrzej Szczepkowicz and Chun-Ming Chang.

*Corresponding author; Electronic address: kjsong@pub.iams.sinica.edu.tw

¹T. E. Madey, C. -H. Nien, K. Pelhos, J. J. Kolodziej, I. M. Abdelrehim, and H.-S. Tao, *Surf. Sci.* **438**, 191 (1999).

²Q. Chen and N. V. Richardson, *Prog. Surf. Sci.* **73**, 59 (2003).

³K. Pelhos, T. E. Madey, and R. Blaszczyszyn, *Surf. Sci.* **426**, 61 (1999).

⁴G. Antczak, T. E. Madey, M. Blaszczyszyn, and R. Blaszczyszyn, *Vacuum* **63**, 43 (2001).

⁵R. Bryl and A. Szczepkowicz, *Appl. Surf. Sci.* **241**, 431 (2005).

⁶T.-Y. Fu, L.-C. Cheng, C.-H. Nien, and T. T. Tsong, *Phys. Rev. B* **64**, 113401 (2001).

⁷H. S. Kuo, I. S. Hwang, T.-Y. Fu, J. Y. Wu, C. C. Chang, and T. T. Tsong, *Nano Lett.* **4**, 2379 (2004).

⁸K.-J. Song, C. Z. Dong, and T. E. Madey, *Langmuir* **7**, 3019 (1991).

⁹J. J. Kolodziej, T. E. Madey, J. W. Keister, and J. E. Rowe, *Phys. Rev. B* **65**, 075413 (2002).

¹⁰J. J. Kolodziej, T. E. Madey, J. W. Keister, and J. E. Rowe, *Phys. Rev. B* **62**, 5150 (2000).

¹¹J. Block, J. J. Kolodziej, J. E. Rowe, T. E. Madey, and E. Schroder, *Thin Solid Films* **428**, 47 (2003).

¹²C.-H. Nien, T. E. Madey, Y. W. Tai, T. C. Leung, J. G. Che, and C. T. Chan, *Phys. Rev. B* **59**, 10335 (1999).

¹³S. P. Chen, *Surf. Sci.* **274**, L619 (1992).

¹⁴J. G. Che, C. T. Chan, C. H. Kuo, and T. C. Leung, *Phys. Rev. Lett.* **79**, 4230 (1997).

¹⁵C. Oleksy, *Surf. Sci.* **549**, 246 (2004).

¹⁶K.-J. Song, W. R. Chen, V. Yeh, Yu-Wen Liao, P. T. Tsao, and M. T. Lin, *Surf. Sci.* **478**, 145 (2001).

¹⁷K.-J. Song, J. C. Lin, M. Y. Lai, and Y. L. Wang, *Surf. Sci.* **327**, 17 (1995).

- ¹⁸A. Szczepkiewicz and R. Bryl, *Surf. Sci.* **559**, L169 (2004).
- ¹⁹C.-H. Nien and T. E. Madey, *Surf. Sci.* **380**, L527 (1997).
- ²⁰S. C. Wang and G. Ehrlich, *Surf. Sci.* **206**, 451 (1988).
- ²¹T.-Y. Fu, L.-C. Cheng, Y.-J. Hwang, and T. T. Tsong, *Surf. Sci.* **507**, 103 (2002).
- ²²D. C. Senft and G. Ehrlich, *Phys. Rev. Lett.* **74**, 294 (1995).
- ²³D. B. Danko, M. Kuchowicz, and J. Kolaczkiwicz, *Surf. Sci.* **552**, 111 (2004).
- ²⁴For one extra atom adsorbed on a perfect bcc surface, the numbers of nearest (N) and next nearest (NN) neighbors are (4,3) on (111) surface, (3,3) on the (112) surface and (2,2) on (110) surface.
- ²⁵K.-J. Song, R. E. Demmin, C. Z. Dong, E. Garfunkel, and T. E. Madey, *Surf. Sci.* **227**, L79 (1990).
- ²⁶K. Pelhos, T. E. Madey, J. B. Hanon, and G. L. Kellogg, *Surf. Rev. Lett.* **6**, 767 (1999).